Chemical Engineering Science 145 (2016) 1–9

Contents lists available at ScienceDirect

Chemical Engineering Science

journal homepage: www.elsevier.com/locate/ces

Use of PLIF to assess the mixing performance of small volume USP 2 apparatus in shear thinning media

Konstantinos Stamatopoulos [a], Federico Alberini [a], Hannah Batchelor [b], Mark J.H. Simmons [a,*]

[a] School of Chemical Engineering, University of Birmingham, Edgbaston, Birmingham B15 2TT, United Kingdom
[b] Pharmacy and Therapeutics Section, Institute of Clinical Sciences, College of Medical and Dental Sciences, Medical School Building, University of Birmingham, Edgbaston, Birmingham B15 2TT, United Kingdom

HIGHLIGHTS

- Use of PLIF images to assess mixing in small volume USP 2 apparatus.
- CoV and areal distribution method gives contradictory results.
- Analysis of striation area distribution is presented for various viscous media.
- Highest mixedness level is mainly located above the blade and close to the wall.
- Guidelines in terms of sampling point are presented for minimum data variability.

ARTICLE INFO

Article history:
Received 9 October 2015
Received in revised form
22 November 2015
Accepted 12 January 2016
Available online 29 January 2016

Keywords:
Small volume USP 2
Areal distribution
Mixing performance
PLIF
Rhodamine-6G
Dissolution

ABSTRACT

Planar Laser Induced Fluorescence (PLIF) was used to assess mixing in small volume USP 2 dissolution apparatus for a range of viscous fluids which mimic gastrointestinal media, especially in the fed state. The release into the media from a specially prepared tablet containing Rhodamine 6G dye was tracked in time and the areal distribution method developed by Alberini et al. (2014a) was implemented to characterise the mixing performance. The distributions of the individual striations for selected mixing levels were also presented. These findings illustrate the poor mixing performance of the apparatus resulting in high variance of the dissolution data when working with viscous media. Analysis of data using CoV gives misleading results for the mixing performance of the small volume USP 2 dissolution apparatus. The results showed that the best mixing was mainly located above the blade and close to the wall, i.e. in the region where intensive motion takes place. This work presents important guidelines and precautions for choosing the proper sampling point for a wide range of liquid viscosities to minimize the variability of the dissolution data.

1. Introduction

The USP 2 dissolution apparatus, which is an agitated mixing device, is the most commonly used piece of equipment for *in vitro* evaluation of solid oral dosage forms. However, several reports have suggested considerable variability, unpredictability and randomness in dissolution profiles obtained from it (Cox et al., 1982, 1983; Qureshi and Shabnam, 2001), even when calibrator tablets are used (Baxter et al., 2005; Kukura et al., 2003).

Recently, the small volume USP 2 apparatus has gained popularity due to the reduced mass of material required, whilst retaining the analytical methodology and discriminatory power of the conventional apparatus (Klein and Shah, 2008). Furthermore, the small volume apparatus may be beneficial in the development of biorelevant methods, particularly for paediatric populations. Although this apparatus is a miniaturised version of the conventional apparatus, there is still a need to analyse the hydrodynamics since the miniaturised systems do not exactly replicate the conditions of the standard paddle system (Klein and Shah, 2008), nor the conditions in the GI tract.

In the pharmaceutical industry, accurate prediction of the *in vivo* biopharmaceutical performance of oral drug formulations is

* Corresponding author. Tel.: +44 121 414 5371.
E-mail address: M.J.Simmons@bham.ac.uk (M.J.H. Simmons).

http://dx.doi.org/10.1016/j.ces.2016.01.032

critical to product and process development. As a part of a general drive to develop predictive *in vitro* models, biorelevant media have been proposed and have evolved over the last decade as a tool for *in vitro* biorelevant dissolution tests (Jantratid et al., 2009). The usefulness of the biorelevant dissolution test is that both media composition and hydrodynamics are taken into consideration. This is essential to provide a baseline for drug and dosage-form performance as well as determining possible food effects on the dissolution and bioavailability of orally dosage forms (Wang et al., 2009).

Studies have shown that food viscosity is one of the physiological parameters that can affect oral drug absorption (Levy and Jusko, 1965; Radwan et al., 2012). To examine this, several authors have conducted drug dissolution and disintegration experiments, which under viscous conditions showed reduced dissolution and disintegration rates (Parojcic et al., 2008; Radwan et al., 2012).

Nevertheless, introducing viscosity into the dissolution test may increase the uncertainty and the variability of the results, since the hydrodynamics of the USP 2 apparatus will change as the flow enters the laminar and transitional regimes, where mixing performance is known to worsen with increasing viscosity.

The characterization of the mixing performance of conventional stirred tanks (as used in the chemical industries) using visualization techniques such as Planar Laser Induced Fluorescence (PLIF), has been extensively investigated under different conditions and using viscous fluids (Busciglio et al., 2014; Cheng et al., 2015; Hu et al., 2010; Zhang et al., 2013). Using this non-intrusive method, qualitative and quantitative evaluation of the mixing performance is possible by tracking the motion of a fluorescent tracer injected into the fluid. Thus, the uniformity of the distribution of the fluorescent dye depends upon the mixing performance of the system.

Regarding the mixing performance of USP 2 apparatus, PLIF has been carried out previously by injecting a fluorescent dye into the vessel at different injection points, followed by observation of mixing patterns in simple buffer solution (Baxter et al., 2005; Kukura et al., 2004). In addition, visualization studies have been performed by examining the dissolution of a salicylic acid tablet containing a phenolphthalein indicator, as a first step in determining the fluid flow patterns in USP 1 and 2 apparatus (Mauger, 2003). These have also been demonstrated using laser Doppler anemometry (Bocanegra et al., 1990). Furthermore, Particle Image Velocimetry (PIV) combined with Computational Fluid Dynamics (CFD) have been used to characterize the flow pattern in a conventional (1 L) USP 2 apparatus dissolution vessel (Baxter et al., 2005; Kukura et al., 2003), revealing a non-uniform velocity field and thus an uneven distribution of shear rates.

Whilst these studies are valuable for highlighting the drawbacks of the USP 2 dissolution apparatus, they do not allow any direct or indirect correlation with the dissolution profile of an active compound. The concern is that they use a method, i.e. PLIF capable of capturing local time-dependent mixing conditions in the USP 2 and yet use a conventional sampling technique for generating dissolution profiles of the targeted drug. Indeed, Kukura et al. (2003, 2004) could not find a significant difference in dissolution profiles of the targeted drug at the different sampling points, although, large fluctuations of the mixing patterns were observed with time (Kukura et al., 2003, 2004). Previous works (Parojcic et al., 2008; Radwan et al., 2012) testing different dosage forms in viscous media did not give any information as to the position of the sample tube to generate the dissolution profile of the tested drug or possible changes in hydrodynamics (e.g. shear rates and/or velocities) or mixing patterns. Thus, there is a need for a study that uses PLIF data generated by capturing images of a fluorescent dye released from compressed tablets, which mimics the release mechanism of the targeted drug. A study which includes sampling location is essential to provide data relevant to the conventional drug dissolution experiments.

It has been recognised that the choice of method or algorithm used to evaluate the mixing performance is of critical importance and that a simple numerical measure based on concentration variance or scale of segregation (Danckwerts, 1952) (obtained after image analysis of the fluid flow) cannot describe the complexity of a flow pattern within a mixer (Alberini et al., 2014a).

Regarding the mixing performance in the USP 2 apparatus, the release of drug and/or dye from a tablet into a viscous medium could reflect a case where a second element is introduced into the fluid and, therefore, segregation area and concentration variance should both be considered. This multi-dimensional analysis of mixing is the basis of the so called areal distribution method (Alberini et al., 2014b). This method was developed to analyse the blending of two fluid components with different apparent viscosities under laminar mixing in a static mixer in which viscous filaments are formed.

Similarly, Stamatopoulos et al. (2015) using the small volume USP 2 apparatus showed that filaments of highly concentrated RH-6G were formed when dye is released in a controlled manner from

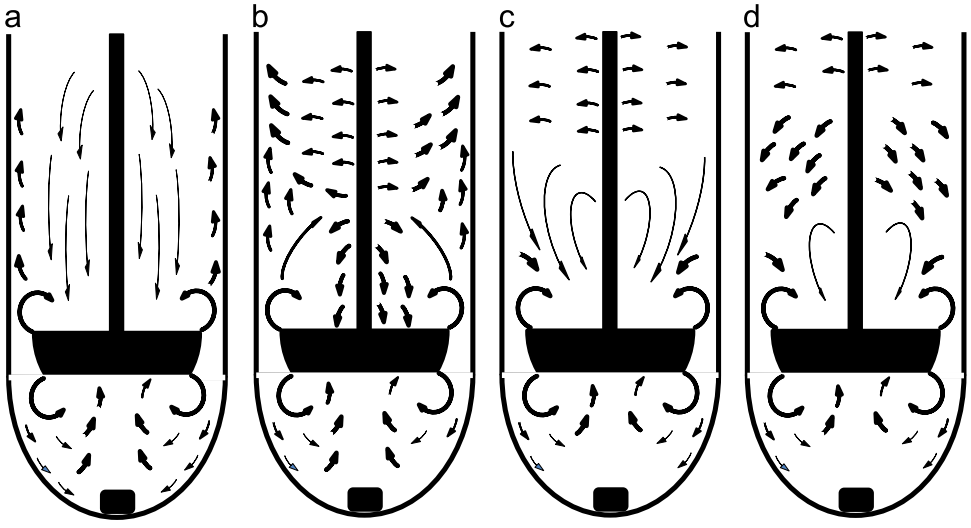

Fig. 1. Schematic representation of the experimental fluid flow patterns within USP2 mini vessel based upon PIV analysis conducted by Stamatopoulos et al. (2015); (a) "simple" buffer, (b) 0.25% NaCMC, (c) 0.50% NaCMC and d) 0.75% NaCMC.

a tablet. They also showed dramatic differences in flow regime as a function of viscosity from PIV measurements (Fig. 1).

Assessing the distribution of the released drug molecules in a viscous media is very important for the performance of the dissolution method. For example, drawing a sample from a "dead zone" may lead to inconsistent dissolution data. This is due to the fact that drug molecules from highly concentrated areas could enter low concentration regions due to flow generated locally by the pumping tube. Thus, whilst CoV enables the range of concentrations to be assessed, it does not consider the local distribution of the dye concentration; the areal distribution method and individual striation methods use both which is a clear advantage.

In this paper, dissolution experiments using a RH-6G impregnated tablet were carried out using the small volume USP 2 apparatus. The distribution of the released RH-6G dye within the small vessel was determined by capturing PLIF images at several time intervals; reflecting the typical sampling process to generate the dissolution profile of the targeted drug. The mixing performance was evaluated in different viscous fluids using CoV, the areal distribution and individual striation methods. This paper examines the effect of the viscosity on the mixing performance of the small volume USP 2 apparatus giving valuable guidelines and precautions for choosing the proper sampling point for a wide range of viscosities to minimize as much as possible the variability of the dissolution data.

2. Materials and methods

2.1. Materials

Sodium carboxymethylcellulose of 90000 ($NaCMC_{90000}$) and 700000 ($NaCMC_{700000}$) molecular weight were purchased from Sigma (St., Louis, USA). Theophylline anhydrous (THE) and potato starch were bought from Acros Organics (Loughborough, UK). Sodium hydroxide, Rhodamine-6G, hydrochloric acid (1 M), silicon dioxide and potassium hydrogen (KH_2PO_4)- and dihydrogen phosphate (K_2HPO_4) were purchased from Sigma (St. Louis, USA).

2.2. Fluids and fluid properties

$NaCMC_{700000}$ was selected as a water-soluble polymer with shear thinning rheology to mimic the shear thinning nature of the chyme (Kong and Singh, 2008). $NaCMC_{700000}$ buffered solutions of 0.25, 0.5 and 0.75% (w/w) were prepared using 0.05 M phosphate buffer pH 7.4 (KH_2PO_4/K_2HPO_4). A pH of 7.4 was selected as a representative pH value for the large intestine. All the tested fluids were deaerated using an ultrasound bath before conducting PLIF experiments.

The rheology of the NaCMC solutions was measured using a Discovery Hybrid Rheometer (TA Instruments – a division of Waters Ltd.) coupled with a 40 mm diameter, 4° cone and plate geometry. The temperature was set to 37 °C using an in-built Peltier plate (set at the same temperature as the USP 2 experiments). The rheology was obtained by performing a shear ramp over a range of shear rates from 0.1–1000 s^{-1} and the data were found to fit the Herschel-Bulkley model.

$$\tau = \tau_Y + K\dot{\gamma}^n \quad (1)$$

Where τ is the shear stress, τ_Y is the yield stress $\dot{\gamma}$ is the shear rate, K is the consistency index and n is the power law exponent. The apparent viscosity, μ_A, can be thus determined by evaluating $\tau/\dot{\gamma}$ at a given value of shear rate. The rheological properties of the experimental fluids are presented in Table 1.

Table 1
Rheological characteristics of the dissolution media employed.

	ρ (kgm^{-3})	τ_0 (Pa)	η ($mPa.s$)	K	n	Re	Regime
"Simple" buffer	1000.10		1		1	1503	Transitional
0.25% NaCMC (w/w)	1017.60	0.03	13.34	0.044	0.85	115	
0.50% NaCMC (w/w)	1020.40	0.18	98.11	0.229	0.72	18	
0.75% NaCMC (w/w)	1024.50	0.76	575.60	0.830	0.58	3	Laminar

2.3. Tablet preparation

A 500 mg tablet was prepared according to the following composition: 50% THE, 44.1% $NaCMC_{90000}$, 4.9% potato starch, 1% silicone dioxide and 0.02% RH-6G. The powders were sieved, mixed for 10 min and compressed at fixed pressure of 980.6 bar using a single die tableting machine (Kilian, Coln, D) fitted with flat-faced 9.8 mm punches (Kistler,Winterthur, CH). The cylindrical tablets had a final weight of 500 ± 25 mg.

2.4. Experimental apparatus: USP 2 mini paddle

A schematic of the small volume USP 2 dissolution apparatus (Dissolution Tester 6000, Antech, UK) used in PLIF experiments is shown in Fig. 2. USP 2 consists of an unbaffled cylindrical and hemispherical bottomed vessel, with an internal diameter of 42 mm. The agitation system consists of a 2-paddle impeller mounted on a shaft with a diameter of 6.3 mm, the length of the top edge of the blade is 30 mm whereas the length of the bottom edge of the blade is 17 mm. The distance from the bottom of the impeller to the bottom of the vessel was 20 mm. The volume of media was 100 mL and the paddle rotational speed was fixed at 50 rpm. All the experiments were performed at 37 °C. The flow regime in the vessel was determined by calculation of the Reynolds number

$$\mathrm{Re} = \frac{\rho N D^2}{\mu_A} \quad (2)$$

where ρ is the fluid density, N is the rotational speed, D is the impeller diameter. The apparent viscosity, μ_A, was estimated using the Metzner-Otto method (Metzner and Otto, 1957) which assumes the shear rate in the vessel is proportional to the impeller speed, thus for a Herschel-Bulkley fluid:

$$\mu_A = \frac{\tau_Y}{k_S N} + K(k_S N)^{n-1} \quad (3)$$

The value of Metzner-Otto constant, k_S, in the above expression was 10 (Edwards et al., 1992). Here, k_S is the proportionality between the average shear rate in the mini vessel and the impeller rotational speed. The calculated values of Re are given in Table 1.

2.5. Analysis of PLIF images

The 2-D PLIF measurements were performed using a TSI PIV system comprised of a 532 nm Nd-YAG laser (Litron NanoPIV) pulsing at 7.4 Hz, and a single TSI Powerview 4MP (2048 × 2048 pixels) 12 bit frame-straddling CCD camera, both controlled using a synchronizer (TSI 610035) attached to a personal computer equipped with TSI Insight 4G software. The spatial resolution of the measurements was 10 μm $pixel^{-1}$. The small volume USP 2 vessel was placed in an acrylic box filled with distilled water in order to eliminate refractive index issues due to vessel curvature as well as keeping a constant temperature of 37 °C by circulating

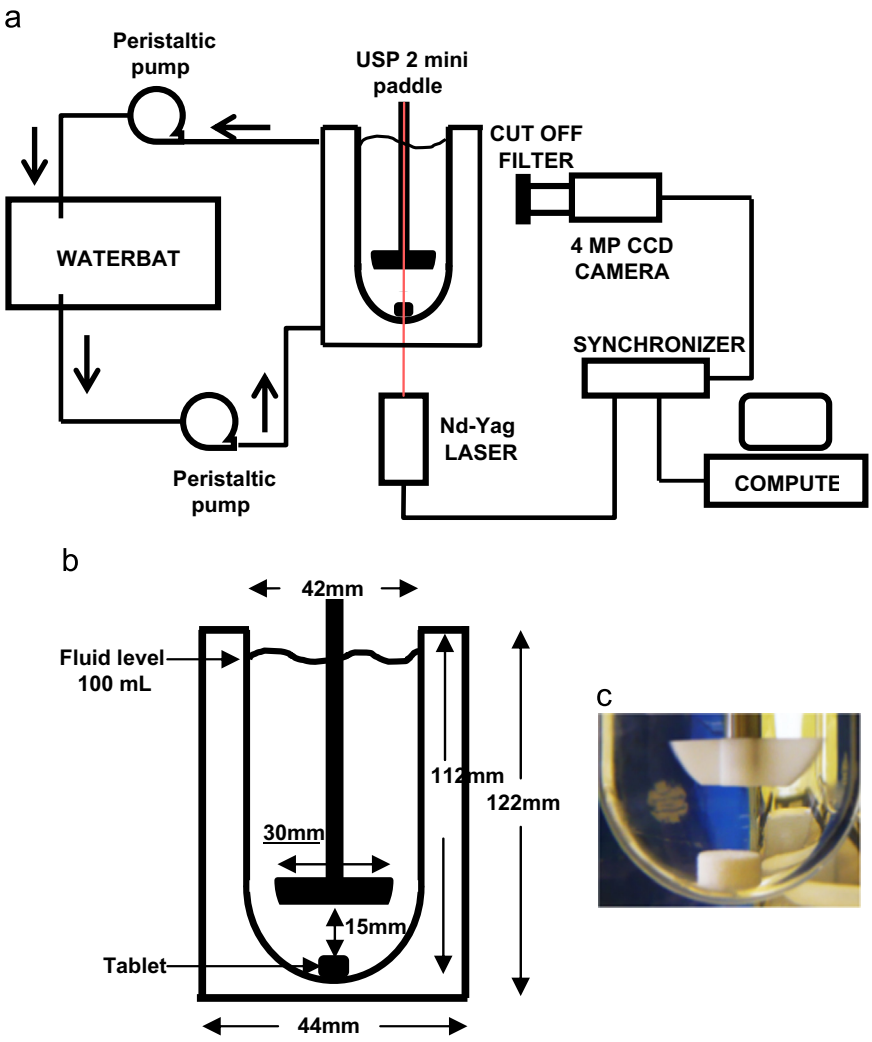

Fig. 2. (a) Overall schematic diagram of the PLIF experimental setup; (b) dimensions of the small vessel USP 2; (c) photo of an USP apparatus 2-bladed impeller used in dissolution experiments.

the fluid in the box through a water bath using a peristaltic pump. The laser sheet was aligned vertically, passing across the diameter of the vessel, i.e. aligned with the impeller shaft along the vessel axis.

A cut-off filter at 545 nm was fitted to the CCD camera to eliminate reflected laser light and to capture only the fluorescent light emitted by the RH-6G (λ=560 nm). The system was calibrated for each solution used at fixed laser power by filling the USP 2 mini vessel with well mixed solutions at concentrations ranging 0–1.0 mg L^{-1}; in steps of 0.1 mg L^{-1}. Potential variation in the laser power was assessed by capturing 50 images for each standard RH-6G solution; values of the relative standard deviation (RSD%) were consistently less than 3.6% and therefore not significant. The region of interest of the illuminated tank is the area where the sampling tube (cannula) is normally inserted as shown in Fig. 3a; the remainder being in shadow due to impingement of the laser sheet on the impeller shaft. Pixel by pixel calibration was developed by taking the average grayscale values over the 50 images. Subsequently, a linear regression over concentration range was performed. The amount of RH-6G incorporated in the tablet was carefully chosen in order the final concentration of the fluorescent dye in the mini vessel to be a maximum of 1 mg L^{-1}. Thus all the grayscale values were within the range of the calibration and below the saturation signal of

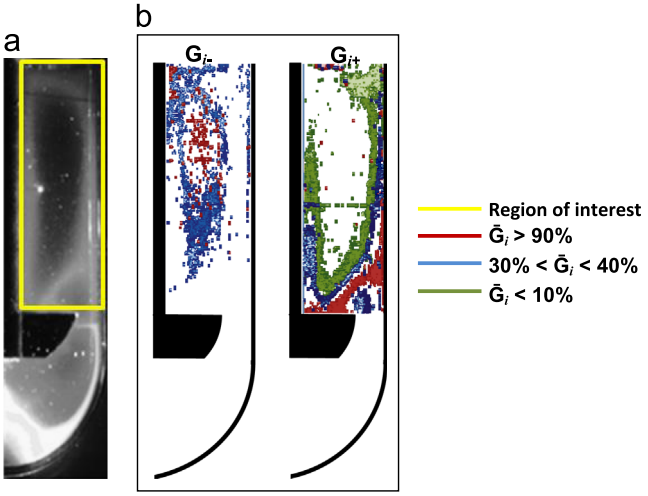

Fig. 3. Development of areal analysis method: (a) raw images with region of interest (yellow line); (b) example of image processing for the 0.5% NaCMC (w/w) with the lower ($Gi-$) and upper ($Gi+$) limits of the individual striations: $G_i > 90\%$ (red labeled pixels), $30\% < G_i < 40\%$ (blue labeled pixels) and $G_i < 10\%$ (green labeled pixels). (For interpretation of the references to color in this figure legend, the reader is referred to the web version of this article.)

the CCD camera. The analysis was carried out using MATLAB (Matlab 7.6.0 R2008a) to produce a calibration matrix.

$$\underline{\underline{C}} = \underline{\underline{a}}\underline{\underline{G}} + \underline{\underline{b}} \quad (4)$$

where $\underline{\underline{C}}$ is the concentration matrix, $\underline{\underline{a}}$ is the matrix of constant values, $\underline{\underline{G}}$ is the matrix of averaged Grayscale values and $\underline{\underline{b}}$ is the matrix of intercept values for the linear regression. The regression was carried out using a standard least-squares method.

The PLIF measurements were conducted by addition of the RH-6G tablet into the bottom of the mini vessel. Dissolution tests (six replicates) were performed in 0.1N HCl solution (gastric conditions) and in 0.05 M phosphate buffer solution (pH 7.4) mimicking the large intestine conditions. The dissolution tests for the viscous media were conducted only at pH 7.4; assuming dewatering of the chyme in large intestine resulting in an increase in viscosity. 10 images were recorded at each predetermined time interval: 0.17 h, 1.0 h, 2.0 h, 6.5 h and finally 20 h.

2.5.1. Areal distribution method

A typical raw image obtained from PLIF performed using viscous media is shown in Fig. 3a. An asymmetric distribution of the fluorescent dye within the USP 2 mini vessel is observable, forming striations with different concentrations of the RH-6G fluorescent dye. The mean value of grayscale in the experimental image ($\overline{G}$) was determined for each time interval at which the PLIF image has been captured. This is based on the fact that only a fraction of the RH-6G dye has been released from the tablet at any given time during the imaging process. Thus, in the current work, $\overline{G}_i$ is the mean value of grayscale in the experimental image corresponds to the fully mixed concentration (C_i) at time i. Here, the fully mixed concentration C_i replaces C_∞, in the areal distribution method (assuming no further release of RH-6G occurs from time i until the time necessary for full homogenisation to occur).

The experimentally determined $\overline{G}_i$ were used to calculate grayscale values corresponding to a given level of mixedness. Then G_i is defined as a percentage of this fully mixed value $\overline{G}_i$. Giving an example, G_i% mixing will correspond to grayscale values of either $G_{i-}=[1-(1-G_i)]\,\overline{G}_i$ or $G_{i+}=[1-(1+G_i)]\,\overline{G}_i$. Thus for 80% mixing, $G_{i-}=0.80\overline{G}_i$ and $G_{i+}=1.2\overline{G}_i$.

Using MATLAB (2008a) and the freeware image analysis tool Image J, the pixels in the image are identified which correspond to $G_{i-} < \overline{G}_i < G_{i+}$, thus corresponding to a mixing intensity of $> G_i$%.

2.5.2. Individual striation method

The work individual striation method was implemented to illustrate indirectly how the mixing performance of USP 2 mini vessel, and therefore the distribution of the dye in the viscous media, affects the reproducibility and hence the variability of the dissolution data of the targeted drug (Alberini et al. 2015b). Thus, identification of individual striations within different ranges of G_i was performed. The individual striations were determined using a MATLAB script which utilizes both the MATLAB image processing toolbox and the DIPimage toolbox developed by the Quantitative Imaging Group at TU Delft (http://www.diplib.org). The image analysis scripts used in this work are available by contacting the corresponding author.

Firstly the image is imported in MATLAB and a rectangular mask is created to identify the region of interest; as shown in Fig. 3a. The area within the mask was chosen since this region is where the cannula is normally placed. Using the value of $\overline{G}_i$, the levels of mixing intensity, G_i, per pixel, are determined as previously (Section 2.5.1). Then the ranges of G_i are defined and for each range, two images are created by MATLAB where only the striations in the range of interest are shown: the first shows all the striations in the range of G_{i-} and the second shows all the striations for G_{i+}. An example of this procedure is shown in Fig. 3b.

The fraction of RH-6G released at time i was determined by normalizing $\overline{G}_i$ values with the G_∞ obtained after the complete release of RH-6G from the tablet; i.e. based on the final PLIF image captured after 22 h dissolution testing and the complete disintegration of the tablet.

2.5.3. Coefficient of variation

The CoV was determined using Eq. (5). N_p is the total number of the pixels in the region of interest, C_i the concentration in each pixel which is proportional to the grayscale value and $\overline{C}$ the concentration which would be expected for complete mixing.

$$CoV = \frac{\sigma}{\overline{C}} = \frac{1}{N_p}\sum_{i}^{N_p}\frac{\sqrt{(C_i-\overline{C})^2}}{\overline{C}} \quad (5)$$

As in areal distribution method, here $\overline{C}$ corresponds to the $\overline{C_i}$ and hence to the $\overline{G}_i$.

3. Results and discussion

3.1. Images obtained from PLIF technique

Fig. 4 shows raw PLIF images captured at predetermined time intervals for each viscous medium. When the viscosity of the medium is increased, different patterns of striations are formed. The dye is concentrated in thin striations, for example in the 0.5% NaCMC (w/w) fluid throughout the dissolution experiment, or in a single thick striation forming a large arc as in the case of the 0.25% NaCMC (w/w) fluid; this striation disappears 2.0 h into the dissolution test.

PIV analysis in the USP 2 mini vessel carried out previously by Stamatopoulos et al. (2015), showed that high velocities occurred mainly around the impeller and along the shaft. The non-uniform mixing results in large gradients of the shear rates in USP 2 vessel (Baxter et al., 2005). As the NaCMC concentration increases, the shear thinning nature of the fluid increases. This implies that in regions where high velocities and thus high velocity gradients occur, the fluid moves significantly whereas in dead zones the fluid will be stagnant. The shear thinning nature of the fluid within the regions of high shear rates will increase leading to inequalities of the viscosity profile throughout the vessel. As a further consequence, striations will form of different size and shape affecting the mixing performance in viscous media.

Examining the PLIF images it seems that the distribution of the dye in USP 2 mini vessel becomes quite uniform in water and in 0.25% NaCMC, especially after 2 h. Although, the difference between grayscale values throughout the USP 2 decreases drastically with time, without image analysis it is impossible to evaluate the mixing performance by eye in the ostensibly uniformly distributed dye in these two media. This is also necessary for the 0.75% NaCMC fluid in which the homogeneity of the dye appears on first glance to be greater than for the 0.5% NaCMC (w/w) fluid.

3.2. Areal distribution method

Fig. 5 shows the distribution of area fraction as a function of level of mixedness, G_i, from the areal distribution method for different viscous media at each predetermined time interval. The level of mixedness was determined for the corresponding normalized fraction ($\overline{G}_i/G_\infty$) of RH-6G released at time i.

The poor mixing performance of USP 2 mini vessel is revealed from multiple levels of mixedness for each dissolved fraction. In particular, comparing the PLIF images of “simple” buffer with the corresponding results from the areal distribution analysis (Fig. 5a), an ostensibly homogeneous distribution of dye would expected

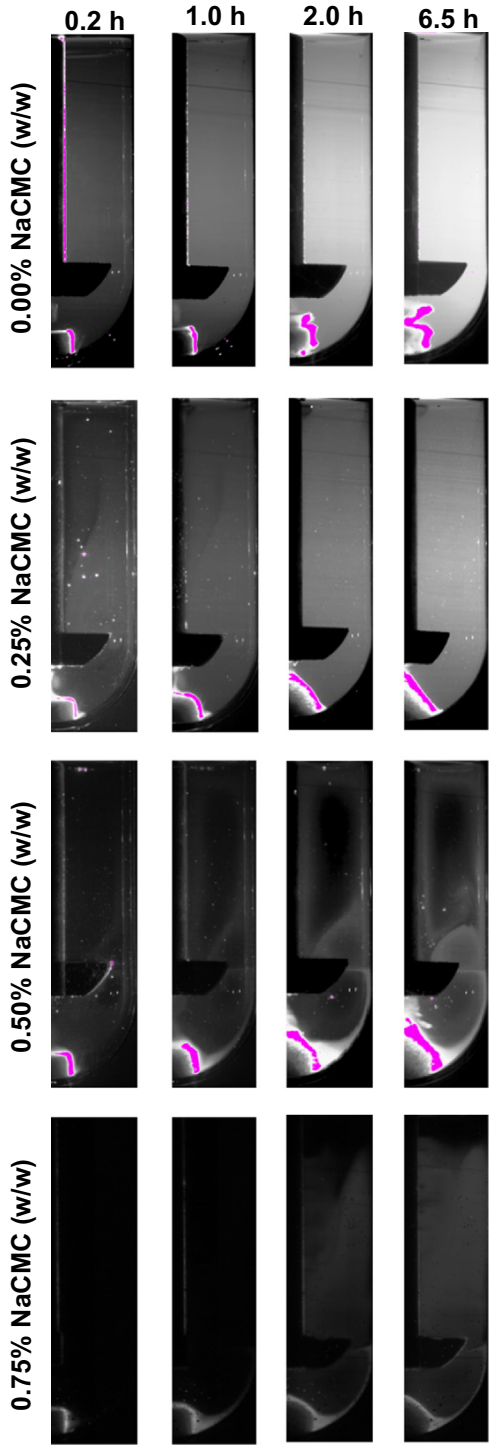

Fig. 4. PLIF images captured at predetermined time interval for water at pH 7.4 (a) and 1.2 (b), whereas (c) 0.25%, (d) 0.5% and (e) 0.75% NaCMC (w/w) buffered (pH 7.4) solution.

giving few different levels of mixedness and the area fraction with $G > 90\%$ to be predominant. This of importance when the dissolution profiles of a drug released from different dosage forms are compared. This is possible only if the standard deviation of the dissolution data of each formulation is $\leq 10\%$. Relatively similar patterns of areal fractions as a function of levels of mixedness were also observed in 0.25% NaCMC (w/w) (Fig. 5b). This spread of the different levels of mixedness becomes even worse in viscous media and in particular for the 0.5% NaCMC medium (Fig. 5c). The areal distribution method reveals here why it was so challenging to compare the dissolution data of the drug and the fluorescence dye as mentioned in Stamatopoulos et al. (2015). Moreover, it is also problematic that in 0.75% NaCMC (w/w) medium (Fig. 5d) the areal fraction is mainly $< 30\%$. This means that the dissolution profile generated under these experimental conditions underestimates the actual release rate of the dye due to the poor mixing performance; this will also increase the variance of the dissolution data.

As expected, the rate of release of RH-6G from the tablet decreases as the viscosity is increased. This is shown in Fig. 6a by plotting the normalized dissolved fraction of RH-6G ($\overline{G}_i/G_\infty$) vs. time. Moreover, the fraction of $G_i > 70\%$ increases and reaches a plateau in "simple" buffer after 2 h whereas the corresponding time for 0.25% NaCMC (w/w), 0.5% NaCMC (w/w) and 0.75% NaCMC (w/w) were 6.0, 7.4 and 8.0 h, respectively (Fig. 6b).

3.3. Individual striation method

The different striations detected by the MATLAB script are identified with different colours. Due to the high number of area fractions used in areal distribution method (as shown in Fig. 5), overlapping of the coloured striations occurred making difficult to distinguish the individual striations. Thus, to show the location and the size of the striations for the corresponding area fractions throughout the USP 2 mini vessel, fixed ranges of area fraction were chosen. Images of the striations detected by the individual striation method are shown for $G < 10\%$, $30\% < G < 40\%$, $70\% < G < 80\%$ and $G > 90\%$ in Fig. 7. The sub-figures for G_{i-} and G_{i+} show the different striations for the lower and upper limits of the selected ranges of level of mixedness, G_i, as described in §2.5.2.

The shape and the size of the striations change as a function of time and hence as function of the released fraction of RH-6G dye, as well as the viscosity of the fluid. Large striations for the upper limit of the selected ranges were observed close to the wall and above the blade, where the mixing is more intense. In "simple" buffer and for the upper limit of the selected ranges, homogeneous zones above the blade were observed, starting from the highest level of mixedness $G_i > 90\%$ (above the blade), and continuing with $70\% < G_i < 80\%$, $30\% < G_i < 40\%$ and $G_i < 10\%$ moving upwards. In addition, the striations in "simple" buffer are more concentrated, occupying small area compared to the striations of the same ranges in the viscous media which are wider and extended from the blade to the top of the mini vessel. With regards to the lower limit of the selected ranges (G_{i-}), striations were detected at the middle of the distance between the blade and the top of the mini vessel for the first 0.17 h of the dissolution experiment in "simple" buffer. At 1 h and 2 h a small striation was detected in the top region of the vessel but not at 6.5 h.

In 0.5% NaCMC (w/w), at 0.17 h, the identified regions of G_{i+} are shown to be extended from the blade to the top of the mini vessel along the wall whereas the regions of G_{i-} are located on the opposite side along the shaft; forming almost a mirror image. This pattern is changed at 2.0 and 6.5 h, where a loop around the region of interest is formed. The lower limits of $70\% < G_i < 80\%$ and $30\% < G_i < 40\%$ are located inside the core of the loop whereas the corresponding upper limit of $30\% < G_i < 40\%$ is outside and around the striation of $G_i < 10\%$. Regarding the upper limits of $G_i > 90\%$ and $70\% < G_i < 80\%$, these striations are located around the circulation zone close to the tip.

In 0.75% NaCMC (w/w) and for 0.17–1.0 h, striations for the $30\% < G_i < 40\%$ and $70\% < G_i < 80\%$ are extended throughout the region of interest whereas a thin line of the $G_i > 90\%$ fraction extends from the blade to the top of the mini vessel and along the shaft. However, at 2.0 h, the striation of $G_i > 90\%$ is limited: a region of $G_{i+} > 90\%$ is located at the connection point of the shaft and the blade whereas G_{i-} is located at the top. The same flow

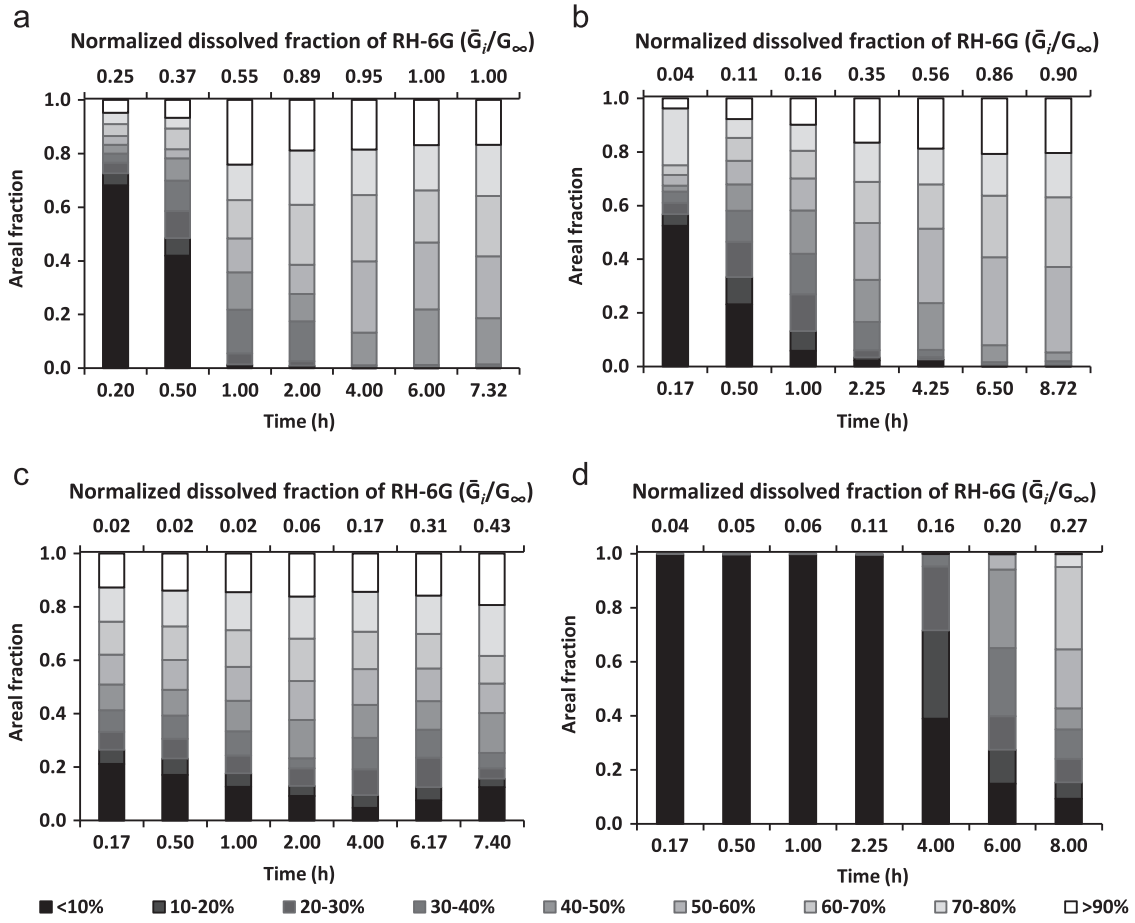

Fig. 5. Bar graph showing discrete areal intensity distributions in viscous media: (a) "simple buffer"; (b) 0.25% NaCMC (w/w); (c) 0.50% NaCMC (w/w); (d) 0.75% NaCMC (w/w).

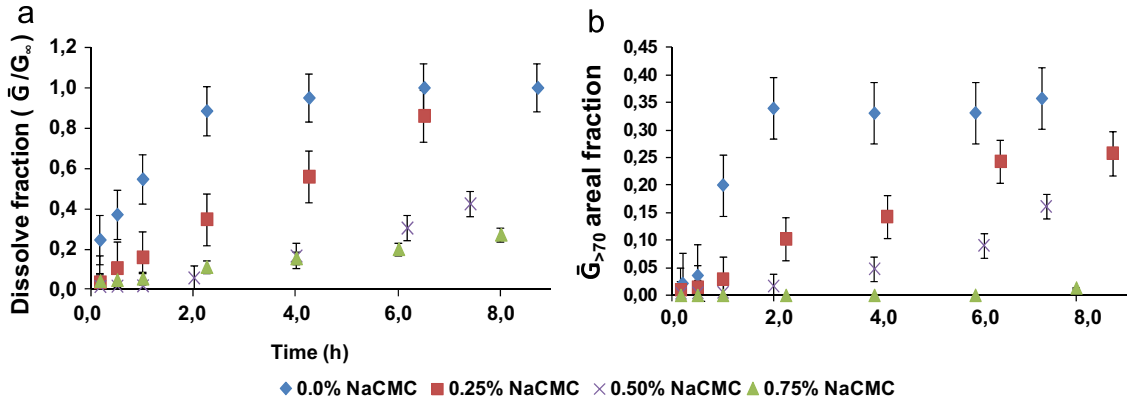

Fig. 6. Evaluation of mixing performance of USP 2 small volume dissolution apparatus. (a) rate of the normalized dissolved fraction of RH-6G ($\bar{G}_i/G_\infty$) released from the tablet and (b) mixing intensity $G_i > 70\%$ as a function of time in different viscous media.

behaviour is also observed for the corresponding upper limit of the other two fractions $30\% < G_i < 40\%$ and $70\% < G_i < 80\%$.

3.4. Coefficient of variation

The mixing performance of small volume USP 2 was also evaluated by calculation of CoV as a function of dissolution time in different viscous media (Fig. 8). As expected, the mixing performance reduces as the viscosity increases. Unlike the areal distribution method, the CoV parameter describes a statistical level of mixing across the whole measurement region. Thus the detail is lost. Characteristic examples are shown for the "simple" buffer, 0.50% NaCMC (w/w) and 0.75% NaCMC (w/w). In the first case a sharp decrease of CoV from 1.0 to 0.4 was observed between 0.2 and 0.5 h dissolution time; implying a 60% mixedness level. However, the areal distribution method showed that the 60–70% fraction consists only the 7% measured area at 0.5 h whereas the fraction $< 10\%$ is 38% of the area (Fig. 5a) – thus a large unmixed area. In the second case, the CoV analysis shows better mixing performance in 0.75% NaCMC (w/w) throughout the dissolution experiment compared with the 0.50% NaCMC (w/w) medium. Nevertheless, areal distribution method showed clearly that the

Fig. 7. Illustration of striations detected using the individual striation method for selected ranges of level of mixedness, G_i, for (a) "simple buffer"; (b) 0.25% NaCMC (w/w); (c) 0.50% NaCMC (w/w); (d) 0.75% NaCMC (w/w).

mixing efficiency is inadequate in the most viscous media, where even after 2.25 h the mixedness fraction of $< 10\%$ is predominant. Thus use of CoV alone may be misleading.

These findings show that individual striation method coupled with areal distribution method is very promising not only to evaluate the mixing performance of small volume USP 2 apparatus and therefore its impact on the reproducibility of the dissolution data, but also to determine the location of the different mixedness levels in the dissolution vessel, via the local distribution of the concentration. This is not possible by consideration of the CoV of the dissolution data alone.

4. Conclusions

The mixing performance of small volume USP 2 apparatus has been determined in shear thinning media from the distribution of a fluorescent dye released from hydrophilic matrix which mimics the dissolution profile of a targeted drug (Stamatopoulos et al., 2015). The areal distribution method presented by Alberini et al. (2014a), in combination with the individual striation method by Alberini et al. (2014b) was used to provide an improved and more detailed measure of the mixing performance according to the level of mixedness, G_i. This is advantageous to determine which region

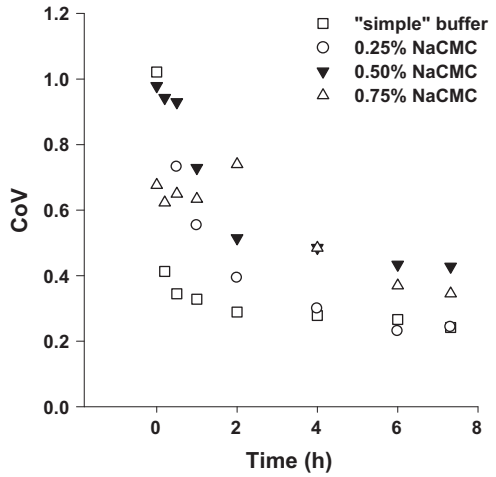

Fig. 8. Time evolution of the coefficient of variation (CoV) as a function of viscosity; (□) "simple" buffer, (○) 0.25% NaCMC (w/w), (▾) 0.50% NaCMC (w/w) and (△) 0.75% NaCMC (w/w).

within the USP 2 mini vessel shows the highest mixing level; something very important in terms of choice of sampling point. Thus, might be possible to minimize the variance of the dissolution data as well as to know in advance the degree of the variability of the data obtained from the selected region. Analysis of data using CoV alone can give misleading results.

Overall, for all measured fluid media, the highest mixedness level is mainly located above the blade and close to the wall, i.e. the region where intensive mixing takes place; therefore the recommendation is that the sample tube (cannula) should be placed in this region.

Acknowledgements

KS is sponsored by an EPSRC (EP/K502984/1) DTP Studentship at the School of Chemical Engineering, the University of Birmingham.

References

Alberini, F., Simmons, M.J.H., Ingram, A., Stitt, E.H., 2014a. Assessment of different methods of analysis to characterise the mixing of shear-thinning fluids in a Kenics KM static mixer using PLIF. Chem. Eng. Sci. 112, 152–169.

Alberini, F., Simmons, M.J.H., Ingram, A., Stitt, E.H., 2014b. Use of an areal distribution of mixing intensity to describe blending of non-newtonian fluids in a kenics KM static mixer using PLIF. AIChE J. 60, 332–342.

Baxter, J.L., Kukura, J., Muzzio, F.J., 2005. Hydrodynamics-induced variability in the USP apparatus II dissolution test. Int. J. Pharm. 292, 17–28.

Bocanegra, L.M., Morris, G.J., Jurewicz, J.T., Mauger, J.W., 1990. Fluid and particle laser doppler velocity measurements and mass transfer predictions for the usp paddle method dissolution apparatus Drug Dev. Ind. Pharm. 16, 1441–1464.

Busciglio, A., Grisafi, F., Scargiali, F., Brucato, A., 2014. Mixing dynamics in uncovered unbaffled stirred tanks. Chem. Eng. J. 254, 210–219.

Cheng, D., Feng, X., Cheng, J., Yang, C., Mao, Z.-S., 2015. Experimental study on the dispersed phase macro-mixing in an immiscible liquid–liquid stirred reactor. Chem. Eng. Sci. 126, 196–203.

Cox, D.C., Wells, C.E., Furman, W.B., Savage, T.S., King, A.C., 1982. Systematic error associated with apparatus 2 of the USP dissolution test II: Effects of deviations in vessel curvature from that of a sphere. J. Pharm. Sci. 71, 395–399.

Cox, D.C., Furman, W.B., Thornton, L.K., Moore, T.W., Jefferson, E.H., 1983. Systematic error associated with apparatus 2 of the USP dissolution test III: limitations of calibrators and the USP suitability test. J. Pharm. Sci. 72, 910–913.

Danckwerts, P.V., 1952. The definition and measurement of some characteristics of mixtures. Appl. Sci. Res. Section A 3, 279–296.

Edwards, M.F., Baker, M.R., Godfrey, J.C., 1992. Chapter 8 – Mixing of liquids in stirred tanks. In: Harnby, N., Edwards, M.F., Nienow, A.W. (Eds.), Mixing in the Process Industries, Second Edition Butterworth-Heinemann, Oxford, pp. 137–158.

Hu, Y., Liu, Z., Yang, J., Jin, Y., Cheng, Y., 2010. Study on the reactive mixing process in an unbaffled stirred tank using planar laser-induced fluorescence (PLIF) technique. Chem. Eng. Sci. 65, 4511–4518.

Jantratid, E., De Maio, V., Ronda, E., Mattavelli, V., Vertzoni, M., Dressman, J.B., 2009. Application of biorelevant dissolution tests to the prediction of in vivo performance of diclofenac sodium from an oral modified-release pellet dosage form. Eur. J. Pharm. Sci. 37, 434–441.

Klein, S., Shah, V., 2008. A standardized mini paddle apparatus as an alternative to the standard paddle. AAPS PharmSciTech 9, 1179–1184.

Kong, F., Singh, R.P., 2008. Disintegration of solid foods in human stomach. J. Food Sci. 73, R67–R80.

Kukura, J., Baxter, J.L., Muzzio, F.J., 2004. Shear distribution and variability in the USP Apparatus 2 under turbulent conditions. Int. J. Pharm. 279, 9–17.

Kukura, J., Arratia, P.E., Szalai, E.S., Muzzio, F.J., 2003. Engineering tools for understanding the hydrodynamics of dissolution tests. Drug Dev. Ind. Pharm. 29, 231–239.

Levy, G., Jusko, W.J., 1965. Effect of viscosity on drug absorption. J. Pharm. Sci. 54, 219–225.

Mauger, J.W., Brockson, R., De, S., Gray, V.A., Robinson, D., 2003. Intrinsic dissolution performance of USP apparatus 2 using modified salicylic acid calibrator tablets: proof of principle Dissol. Technol. 10, 6.

Metzner, A.B., Otto, R.E., 1957. Agitation of non-Newtonian fluids. AIChE J. 3, 3–10.

Parojcic, J., Vasiljevic, D., Ibric, S., Djuric, Z., 2008. Tablet disintegration and drug dissolution in viscous media: paracetamol IR tablets. Int. J. Pharm. 355, 93–99.

Wang, Qingxi, Fotaki, Nikoletta, Mao, Yun, 2009. Biorelevant dissolution: methodology and application in drug development. Dissol. Technol. 6–12.

Qureshi, S.A., Shabnam, J., 2001. Cause of high variability in drug dissolution testing and its impact on setting tolerances. Eur. J. Pharm. Sci. 12, 271–276.

Radwan, A., Amidon, G.L., Langguth, P., 2012. Mechanistic investigation of food effect on disintegration and dissolution of BCS class III compound solid formulations: the importance of viscosity. Biopharm. Drug Dispos. 33, 403–416.

Stamatopoulos, K., Batchelor, H.K., Alberini, F., Ramsay, J., Simmons, M.J., 2015. Understanding the impact of media viscosity on dissolution of a highly water soluble drug within a USP 2 mini vessel dissolution apparatus using an optical planar induced fluorescence (PLIF) method. Int. J. Pharm. 495, 362–373.

Zhang, M., Hu, Y., Wang, W., Shao, T., Cheng, Y., 2013. Intensification of viscous fluid mixing in eccentric stirred tank systems. Chem. Eng. Process.: Process Intensif. 66, 36–43.